1,3-Dipolar cycloaddition to the Fe–N=C fragment XVI. [1] Reactivity of Fe(alkyl-NC)₃(ⁱPr-DAB) complexes towards aromatic isothiocyanates as dipolarophiles. Insertion of isothiocyanate into the Fe–N bond

Nantko Feiken [a], Hans-Werner Frühauf [a,*], Kees Vrieze [a], Nora Veldman [b], Anthony L. Spek [b]

[a] *Laboratorium voor Anorganische Chemie, J.H. van 't Hoff Instituut, Universiteit van Amsterdam, Nieuwe Achtergracht 166, 1018 WV Amsterdam, Netherlands*

[b] *Bijvoet Center for Biomolecular Research, Vakgroep Kristal-en structuurchemie, Universiteit Utrecht, Padualaan 8, 3584 CH Utrecht, Netherlands*

Received 29 August 1995

Abstract

The reaction of para-substituted phenyl isothiocyanates (R^3-C_6H_4-NCS; R^3=H (a), Me (b), OMe (c), NO_2 (d)) with Fe(R^2-NC)₃(ⁱPr-DAB) (7) (R^2 =ᵗBu or ᶜHex) leads in a 1,3-dipolar cycloaddition reaction to novel [3.2.0] bicyclic compounds 10 into which two isothiocyanate molecules have been incorporated. A crystal structure determination revealed the unexpected insertion of an isothiocyanate via its C=S moiety and the lack of coordination of the unreacted imine nitrogen atom. Variable temperature NMR experiments showed a dynamic behaviour of 10, which involves interchanging coordination of the amino- and the imine nitrogen atoms to the iron atom.

Complex 10cy is converted on silica gel to another complex 11cy. The structure of complex 11cy has been tentatively assigned, based on stoichiometry and spectroscopic properties. Probably two isothiocyanate molecules (c) have been cycloadded across both C=N–Fe moieties in complex 7y.

Keywords: Iron; Cycloaddition; Isothiocyanates; Crystal structure; Diimine; Isocyanide

1. Introduction

In previous papers of this series we described the 1,3-dipolar cycloaddition reactions of $M(CO)_{3-n}$(CNR^2)$_n$(R^1-DAB) (M = Fe, Ru; n = 0, 1 and 3) [2] complexes with unsaturated organic substrates (see Scheme 1) [1–8]. The product selectivity of these reactions depends on the ligands coordinated to the metal as well as the substitional pattern of the DAB-ligand and the dipolarophile.

The initial [2.2.1] bicyclic adduct 2 could never be observed in the iron systems, because of the very fast consecutive reaction steps giving either 4 by insertion of CO or aryl-isocyanide, or, in the cases of L_1–L_3 = alkyl-isocyanide, giving double cycloaddition products 3 with dimethyl acetylene dicarboxylate.

In this investigation we use Fe(alkyl-NC)₃(ⁱPr-DAB) as 1,3-dipolar substrate and aryl-isothiocyanate as dipolarophiles. This combination is not compatible with either reaction pathway in Scheme 1, and is chosen to probe alternative reaction pathways of the system. Three alkyl-isocyanide ligands at the iron centre result in a very reactive Fe–N=C 1,3-dipole; however, they do not insert into the Fe–N bond after the initial cycloaddition [4,5]. The system was therefore expected to unveil previously inaccessible reaction channels.

---

[1] Part XV: M. van Wijnkoop, P.P.M. de Lange, H.-W. Frühauf, K. Vrieze, W.J.J. Smeets and A.L. Spek, *Organometallics*, 14 (1995) 4781–4791.

* Corresponding author.

[2] The 1,4-diaza-1,3-butadienes of formula R^1N=CH–CH=NR^1 are abbreviated as R^1-DAB.

2. Results and discussion

2.1. General

The complexes and the employed dipolarophiles and ligands are shown in Scheme 2. The type of complex is identified by Arabic numbers. The different para-substituents of the isothiocyanates are differentiated by the letters a–d, whereas the isocyanides are denoted by the letters x and y.

2.2. Reactivity

In situ prepared solutions of $Fe(R^2-NC)_3(R^1-DAB)$ (7) in hexane react at low temperature with different para-substituted phenylisothiocyanates in a HOMO controlled [9,10] oxidative 1,3-dipolar cycloaddition reaction giving the respective [3.2.0] bicyclic compounds 10 (see Scheme 2) in isolated yields of 30–50% after crystallization from hexane–Et_2O. Evaporation of the solvent, immediately after the cycloaddition reaction, showed (^1H NMR) that complexes 10 are formed as major products, but that also several unidentified side products are formed in low yields.
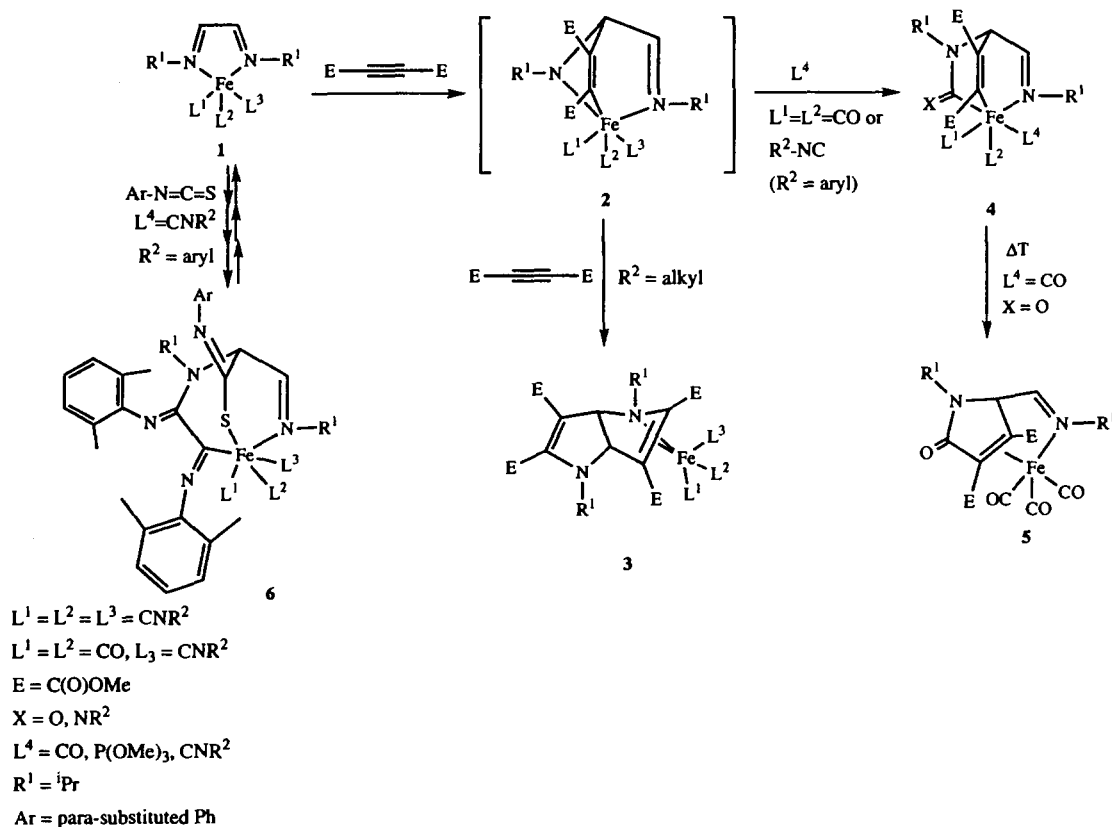
In a previous paper we reported on 1,3-dipolar cycloaddition reactions of para-substituted phenyl isothio-

cyanates as dipolarophiles [8] across the Fe–N=C fragment of ($^iPr-N=CH-CH=N-^iPr)FeL_3$ with L = 2,6-xylyl isocyanide. The cycloadducts in that case were isocyanide inserted products.

Earlier we found that alkyl isocyanides attached to the iron atom [4,5] raised the reactivity of the 1,3-dipole by raising the energy level of the HOMO of the 1,3-dipole. With DMAD as dipolarophile, double cycloaddition products were formed, without insertion of one of the terminally coordinated isocyanide ligands. Insertion of alkyl isocyanide into the N–Fe bond was never observed.

Again, in the present investigation, the alkyl isocyanide ligands do not insert into the Fe–N bond after the cycloaddition step, but instead the C=S group of a dipolarophile molecule (isothiocyanate) is inserted. The possibility of more than one isothiocyanate insertion cannot be excluded; however the yields of any formed by-products are too low (vide supra) to be identified. It is not very likely that the isothiocyanate directly inserts into the Fe–N bond of intermediate 8, i.e. without pre-coordination to the metal atom. The following points therefore have to be considered and will be discussed in that order.

(i) How is an open site created to allow for pre-coordination of the isothiocyanate?

$L^1 = L^2 = L^3 = CNR^2$

$L^1 = L^2 = CO, L_3 = CNR^2$

$E = C(O)OMe$

$X = O, NR^2$

$L^4 = CO, P(OMe)_3, CNR^2$

$R^1 = {}^iPr$

Ar = para-substituted Ph

Scheme 1. Reaction steps in the cycloaddition reaction of DMAD and Ar–N=C=S to the Fe–N=C fragment in complexes $Fe(CO)_{3-n}(R^2-NC)_n(R^1-DAB)$ ($n = 0, 1, 3$).
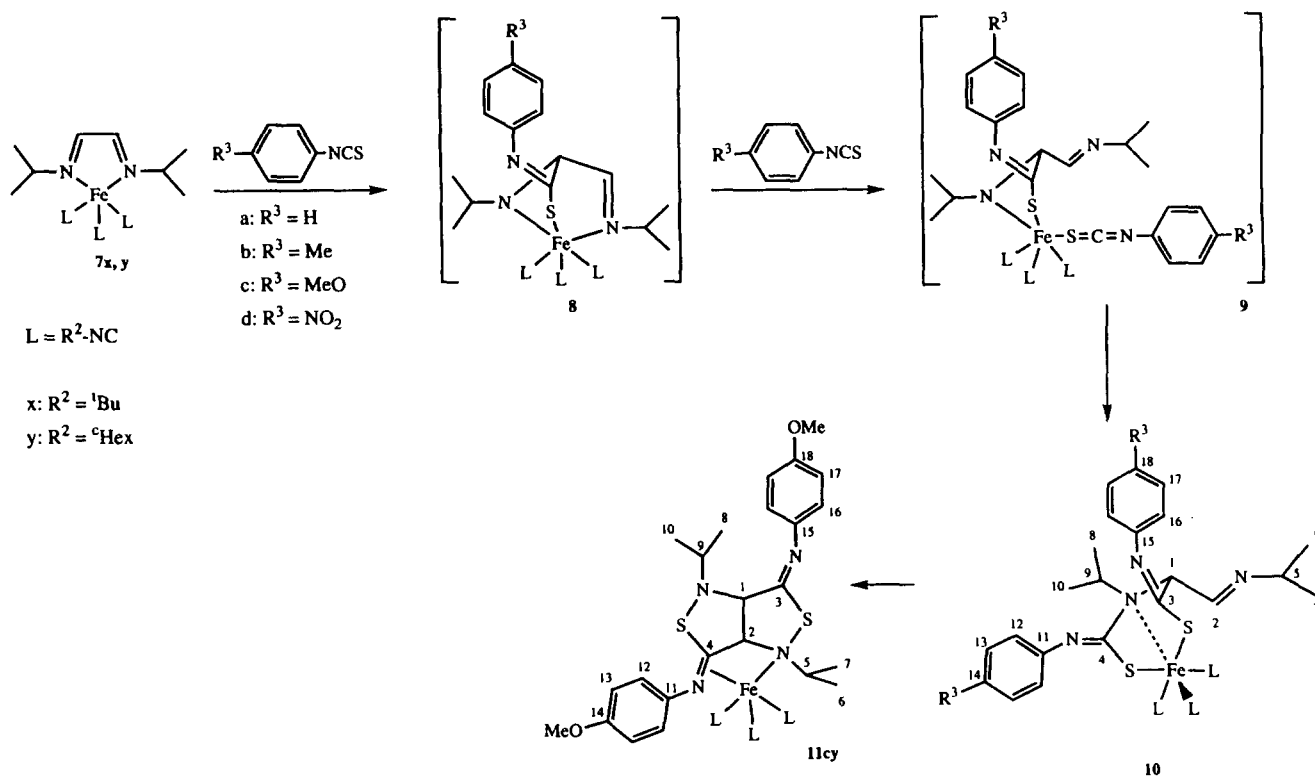
Scheme 2. Proposed mechanism for the 1,3-dipolar cycloaddition of Fe(R^2-NC)$_3$(R^1-DAB) (7) to R^3-Ph-NCS.

(ii) What would be the most likely way for the isothiocyanate to approach and to coordinate to the metal?

(iii) In which way does S=C=N-R insert, i.e. with its C=N- or the C=S-group?

(i) The most likely way to generate an open site in the initial cycloadduct (intermediate **8**) is by decoordination of the imine N-atom. The unchanged imine-arm of the former α-diimine ligand in **8** may show hemilabile behaviour, opening up a coordination site for the isothiocyanate which then immediately reacts further. The on/off movement of the imine-arm in complexes **10**, which explains their dynamic behaviour on the NMR time scale (vide infra), demonstrates such hemilabile behaviour. Prior to having had a direct indication of this hemilabile behaviour it was clear that there is hardly any π-backbonding (from the Fe^{II} atom into the π*-orbital of the isolated imine C=N group) which would reinforce the Fe-N$_{imine}$ bond strength and increase the C=N length. This is indicated by X-ray structural investigations which show a bond length for Fe-N$_{imine}$ of 2.030(3) Å, and a very short C=N bond length [2] of 1.272(4) Å in a [2.2.1] bicyclic structure analogous to **8**, or for Ru-N$_{imine}$ of 2.126(3) Å and C=N of 1.272(6) Å in the Ru(CO)$_3$ analogue [3] of **8**. Comparable bond lengths are also found in [2.2.2] bicyclic structures [1,8] as in **4**.

To test if the isothiocyanates can act as an additional ligand L' (Scheme 1) we have carried out the 1,3-di-

polar cycloaddition reaction of Fe(^{i}Pr-DAB)(CO)$_3$ with DMAD in the presence of one equivalent of aryl-isothiocyanate. Only decomposition products were observed in these cases. Probably the coordination of the aryl isothiocyanates by the sulphur atom or by the C=S moiety is too weak to stabilize the [2.2.2] bicyclic complex. In contrast to the tricarbonyl case, the present bicyclic complex **9** can immediately react further
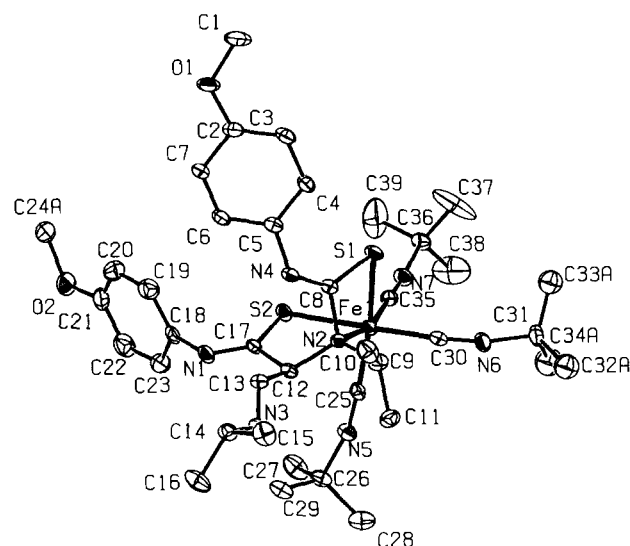

Fig. 1. An ORTEP [16] plot of **10cx** at 30% probability level; hydrogen atoms and the minor disorder parts were left out for clarity.

through insertion into the Fe–N bond of the weakly bonded isothiocyanate.

In order to test if CO can competitively insert in the

Fe–N bond in **8**, the cycloaddition reaction was carried out under an atmosphere of CO. However, in these cases no products were found other than those given in

Table 1
Final coordinates and equivalent isotropic thermal parameters of complex **10cx** (e.s.d. values in parentheses)

Atom	x	y	z	U(eq) (Å)
Fe	0.72634(6)	0.46753(5)	0.25843(4)	0.0282(2)
S(1)	0.89391(10)	0.39678(9)	0.23330(9)	0.0358(4)
S(2)	0.65820(11)	0.36791(9)	0.37088(8)	0.0338(4)
O(1)	1.0566(3)	−0.0179(3)	0.3244(3)	0.0662(16)
O(2)	0.4679(4)	0.1658(3)	0.7100(3)	0.0625(14)
N(1)	0.4691(3)	0.1926(3)	0.3356(3)	0.0391(14)
N(2)	0.6541(3)	0.3296(3)	0.1722(2)	0.0269(12)
N(3)	0.3658(3)	0.1462(3)	0.0998(3)	0.0319(12)
N(4)	0.7395(3)	0.1974(3)	0.2008(3)	0.0305(12)
N(5)	0.4743(4)	0.5109(3)	0.2727(3)	0.0379(14)
N(6)	0.8296(4)	0.6145(3)	0.1289(3)	0.0407(14)
N(7)	0.8863(4)	0.6337(3)	0.3991(3)	0.0390(14)
C(1)	1.1908(5)	0.0197(5)	0.3329(5)	0.080(3)
C(2)	0.9872(4)	0.0429(4)	0.2933(4)	0.0421(19)
C(3)	1.0372(4)	0.1249(4)	0.2492(4)	0.0420(18)
C(4)	0.9580(4)	0.1798(4)	0.2189(3)	0.0373(16)
C(5)	0.8288(4)	0.1515(4)	0.2332(3)	0.0326(16)
C(6)	0.7815(4)	0.0677(4)	0.2762(3)	0.0381(16)
C(7)	0.8588(4)	0.0135(4)	0.3070(4)	0.0433(18)
C(8)	0.7625(4)	0.2926(3)	0.1996(3)	0.0285(14)
C(9)	0.6511(5)	0.3405(4)	0.0711(3)	0.0390(17)
C(10)	0.6579(5)	0.2507(4)	0.0075(4)	0.0550(19)
C(11)	0.5428(5)	0.3820(4)	0.0412(3)	0.0435(17)
C(12)	0.5285(4)	0.2694(3)	0.2030(3)	0.0285(16)
C(13)	0.4656(4)	0.1638(3)	0.1529(3)	0.0299(16)
C(14)	0.3123(4)	0.0416(4)	0.0537(3)	0.0374(17)
C(15)	0.3491(6)	0.0357(4)	−0.0432(4)	0.056(2)
C(16)	0.1676(5)	0.0090(5)	0.0535(5)	0.065(2)
C(17)	0.5445(4)	0.2671(3)	0.3054(3)	0.0285(16)
C(18)	0.4744(4)	0.1903(4)	0.4312(3)	0.0389(16)
C(19)	0.5469(5)	0.1379(4)	0.4721(4)	0.054(2)
C(20)	0.5489(6)	0.1297(5)	0.5635(4)	0.059(2)
C(21)	0.4736(5)	0.1716(5)	0.6176(4)	0.0552(19)
C(22)	0.3996(6)	0.2247(5)	0.5791(4)	0.061(3)
C(23)	0.4008(5)	0.2342(4)	0.4865(4)	0.0517(19)
C(24A) [a]	0.5571(7)	0.1141(6)	0.7493(5)	0.056(3)
C(24B) [a]	0.390(2)	0.2238(17)	0.7677(16)	0.073(8)
C(25)	0.5739(4)	0.4979(3)	0.2673(3)	0.0321(17)
C(26)	0.3415(4)	0.5018(4)	0.2897(4)	0.0418(17)
C(27)	0.3392(5)	0.5306(5)	0.3919(4)	0.062(2)
C(28)	0.2974(6)	0.5743(5)	0.2348(5)	0.072(3)
C(29)	0.2648(5)	0.3924(4)	0.2586(4)	0.051(2)
C(30)	0.7841(4)	0.5537(4)	0.1748(3)	0.0312(16)
C(31)	0.9092(5)	0.6949(4)	0.0898(4)	0.069(2)
C(32A) [a]	0.8733(9)	0.6977(8)	−0.0058(5)	0.071(4)
C(32B) [a]	0.9642(16)	0.6283(12)	0.0100(9)	0.114(9)
C(33A) [a]	1.0448(7)	0.7134(8)	0.1208(7)	0.067(3)
C(33B) [a]	1.0277(10)	0.7501(10)	0.1502(9)	0.062(5)
C(34A) [a]	0.8703(10)	0.7921(7)	0.1437(7)	0.090(4)
C(34B) [a]	0.8474(15)	0.7536(11)	0.0384(12)	0.117(9)
C(35)	0.8200(4)	0.5698(3)	0.3464(3)	0.0332(16)
C(36)	0.9898(4)	0.7037(4)	0.4613(3)	0.0373(17)
C(37)	1.1089(6)	0.7119(8)	0.4189(6)	0.142(5)
C(38)	0.9661(8)	0.8049(5)	0.4722(7)	0.114(4)
C(39)	0.9887(9)	0.6647(7)	0.5497(5)	0.151(5)

[a] Sites have a population less than 1.0.
U(eq) = 1/3 of the trace of the orthogonalized U.

Scheme 2. This means that in the present reactions the stabilization by a subsequent insertion of an isothiocyanate molecule is preferred over the interaction of CO with the [2.2.1] bicyclic intermediates **8**. When the cycloaddition reaction was carried out under an atmosphere of CO and only one (instead of four) equivalents of the arylisothiocyanates, only decomposition products were found. Stirring complexes **10** under CO showed that CO is not incorporated (cf. Scheme 2), e.g. by a decoordination of the amino nitrogen and a subsequent coordination of CO to the iron centre, or by insertion of CO in the Fe–S bond. This is quite unexpected, because the four-membered ring formed by the amino-N, C(4), S and Fe should be very strained. The strain, apparently cannot be released by reaction with CO. Cámpora et al. [11] reported the reaction of CO with a nickel complex containing a Ni–S bond, formed by the reaction with an isothiocyanate. They found CO-inserted organic products in these cases; however, the CO did not insert into the Ni–S bond.

(ii) Mealli et al. [12] studied the bonding to transition-metal fragments of hetereoallene type molecules such as CS_2 and CO_2 using extended Hückel methods. A linear CX_2 molecule can approach a transition-metal by either end-on η^1 approach or by a side-on η^2 approach, both leading finally to an η^2 coordination of such a molecule. Their calculations showed that a reac-

tion path by end-on approach is energetically more favourable, although the energy difference is small (only a few kilocalories per mole preference is calculated). We therefore assume that in our case the incoming isothiocyanate coordinates first via its terminal sulphur atom. Apart from such a theoretical description we think that another approach than via the sulphur atom of the isothiocyanate is not possible for steric reasons.

(iii) The η^1-S coordination of the isothiocyanate should create sufficient positive charge at the neighbouring carbon atom so that it will be immediately attacked nucleophilically by the lone pair of the amido nitrogen, i.e. we have a (migratory) insertion of the C=S moiety into the Fe–N$_{amido}$ bond which is also apparant from the X-ray structure determination of **10cx**. In the literature, however, at least one example is reported [13] where not the C=S but rather the N=C moiety of an isothiocyanate is inserted into a Re–C bond of a di-rhenium complex with a bridging alkyne ligand. In the product, the sulphur atom was coordinated to one of the rhenium atoms.

Complex **11cy** is a rearrangement product of complex **10cy** and was obtained on attempts to purify **10cy** by column chromatography on silanized silica gel. The role of the silanized silica is unknown; probably, silica has acted as a reactive surface or as a heterogeneous catalyst for the conversion of **10cy** to **11cy**. Other

Table 2
Bond distances (Å) of Complex **10cx** (e.s.d. values in parentheses)

Fe–S(1)	2.3363(14)	C(2)–C(7)	1.378(7)
Fe–S(2)	2.3006(14)	C(3)–C(4)	1.393(7)
Fe–N(2)	2.089(4)	C(4)–C(5)	1.388(7)
Fe–C(25)	1.837(5)	C(5)–C(6)	1.373(7)
Fe–C(30)	1.829(5)	C(6)–C(7)	1.372(7)
Fe–C(35)	1.829(4)	C(9)–C(10)	1.491(8)
S(1)–C(8)	1.725(4)	C(9)–C(11)	1.522(8)
S(2)–C(17)	1.732(4)	C(12)–C(13)	1.511(6)
O(1)–C(1)	1.403(7)	C(12)–C(17)	1.515(6)
O(1)–C(2)	1.383(6)	C(14)–C(15)	1.503(7)
O(2)–C(21)	1.377(7)	C(14)–C(16)	1.515(8)
O(2)–C(24A)	1.494(9)	C(18)–C(19)	1.377(7)
O(2)–C(24B)	1.55(2)	C(18)–C(23)	1.383(7)
N(1)–C(17)	1.268(6)	C(19)–C(20)	1.364(8)
N(1)–C(18)	1.411(6)	C(20)–C(21)	1.372(9)
N(2)–C(8)	1.473(6)	C(21)–C(22)	1.380(9)
N(2)–C(9)	1.514(5)	C(22)–C(23)	1.387(8)
N(2)–C(12)	1.514(6)	C(26)–C(27)	1.516(8)
N(3)–C(13)	1.254(6)	C(26)–C(28)	1.524(9)
N(3)–C(14)	1.468(7)	C(26)–C(29)	1.513(8)
N(4)–C(5)	1.399(6)	C(31)–C(32A)	1.450(10)
N(4)–C(8)	1.275(6)	C(31)–C(33A)	1.467(10)
N(5)–C(25)	1.158(6)	C(31)–C(34A)	1.655(12)
N(5)–C(26)	1.458(7)	C(31)–C(32B)	1.654(16)
N(6)–C(30)	1.161(7)	C(31)–C(33B)	1.486(14)
N(6)–C(31)	1.409(7)	C(31)–C(34B)	1.447(17)
N(7)–C(35)	1.152(6)	C(36)–C(37)	1.455(9)
N(7)–C(36)	1.456(6)	C(36)–C(38)	1.490(9)
C(2)–C(3)	1.368(8)	C(36)–C(39)	1.467(9)

attempts to obtain **11cy**, e.g. by stirring of **10cy** in solution (THF, CH_2Cl_2 or toluene) for several days, or by heating **10cy** in THF, led only to decomposition products. **11cy** is exclusively formed with isothiocyanate **c** and with isocyanide **y**. This compound, in which two dipolarophilic isothiocyanates have probably added with their C=S bonds across both Fe–N=C moieties of complex **7** with consecutive reductive eliminations, shows a great spectroscopic resemblance with the earlier reported double cycloaddition products [4,5] formed with DMAD and **7**. For complex **11cy** we therefore tentatively assign the structure shown in

Scheme 2, i.e. a $Fe(^cHex-NC)_3$ fragment coordinated to an isothiazolo[3,4-c] isothiazol skeleton of which both rings have an exocyclic imine group. Unfortunately, all efforts to crystallize **11cy** in order to determine its X-ray crystal structure failed. Also, decomplexation attempts in order to isolate and further characterize the organic part of **11cy** failed.

2.3. Crystal structure of complex 10cx

The crystal structure of complex **10cx**, together with the atomic numbering is shown in Fig. 1. Tables 1–3 give the atomic coordinates, bond lengths and angles.

Table 3
Bond angles (deg) of complex **10cx** (e.s.d. values in parentheses)

S(1)–Fe–S(2)	91.67(5)	C(25)–N(5)–C(26)	164.7(5)
S(1)–Fe–N(2)	71.39(10)	C(30)–N(6)–C(31)	166.3(5)
S(1)–Fe–C(25)	168.41(14)	C(35)–N(7)–C(36)	168.2(5)
S(1)–Fe–C(30)	89.50(16)	O(1)–C(2)–C(3)	124.4(4)
S(1)–Fe–C(35)	94.67(15)	O(1)–C(2)–C(7)	115.1(5)
S(2)–Fe–N(2)	82.87(10)	C(3)–C(2)–C(7)	120.5(5)
S(2)–Fe–C(25)	84.53(14)	C(2)–C(3)–C(4)	119.7(4)
S(2)–Fe–C(30)	176.33(15)	C(3)–C(4)–C(5)	120.2(5)
S(2)–Fe–C(35)	89.69(14)	N(4)–C(5)–C(4)	124.8(5)
N(2)–Fe–C(25)	97.24(17)	N(4)–C(5)–C(6)	116.5(4)
N(2)–Fe–C(30)	100.79(18)	C(4)–C(5)–C(6)	118.4(5)
N(2)–Fe–C(35)	163.89(17)	C(5)–C(6)–C(7)	121.9(5)
C(25)–Fe–C(30)	95.0(2)	C(2)–C(7)–C(6)	119.2(5)
C(25)–Fe–C(35)	96.2(2)	S(1)–C(8)–N(2)	107.9(3)
C(30)–Fe–C(35)	86.8(2)	S(1)–C(8)–N(4)	134.5(4)
Fe–S(1)–C(8)	78.92(15)	N(2)–C(8)–N(4)	117.3(4)
Fe–S(2)–C(17)	99.57(15)	N(2)–C(9)–C(10)	116.1(4)
C(1)–O(1)–C(2)	118.0(4)	N(2)–C(9)–C(11)	111.7(4)
C(21)–O(2)–C(24A)	114.3(5)	C(10)–C(9)–C(11)	112.9(4)
C(21)–O(2)–C(24B)	120.6(9)	N(2)–C(12)–C(13)	117.8(4)
C(17)–N(1)–C(18)	118.5(4)	N(2)–C(12)–C(17)	109.3(3)
Fe–N(2)–C(8)	93.2(2)	C(13)–C(12)–C(17)	110.5(3)
Fe–N(2)–C(9)	113.7(3)	N(3)–C(13)–C(12)	120.3(4)
Fe–N(2)–C(12)	109.9(2)	N(3)–C(14)–C(15)	109.2(4)
C(8)–N(2)–C(9)	110.3(3)	N(3)–C(14)–C(16)	110.0(4)
C(8)–N(2)–C(12)	112.8(3)	C(15)–C(14)–C(16)	109.9(5)
C(9)–N(2)–C(12)	115.0(3)	S(2)–C(17)–N(1)	126.0(4)
C(13)–N(3)–C(14)	116.4(4)	S(2)–C(17)–C(12)	117.7(3)
C(5)–N(4)–C(8)	124.3(4)	N(1)–C(17)–C(12)	116.3(4)
N(1)–C(18)–C(19)	120.9(4)	N(6)–C(31)–C(33A)	111.6(6)
N(1)–C(18)–C(23)	121.7(4)	N(6)–C(31)–C(34A)	100.3(5)
C(19)–C(18)–C(23)	117.3(5)	N(6)–C(31)–C(32B)	99.2(7)
C(18)–C(19)–C(20)	122.4(5)	N(6)–C(31)–C(33B)	112.5(7)
C(19)–C(20)–C(21)	120.0(6)	N(6)–C(31)–C(34B)	117.4(8)
O(2)–C(21)–C(20)	124.1(6)	C(32A)–C(31)–C(33A)	119.3(7)
O(2)–C(21)–C(22)	116.6(5)	C(32A)–C(31)–C(34A)	103.1(6)
C(20)–C(21)–C(22)	119.3(6)	C(33A)–C(31)–C(34A)	104.4(6)
C(21)–C(22)–C(23)	120.0(6)	C(32B)–C(31)–C(33B)	102.1(8)
C(18)–C(23)–C(22)	121.1(5)	C(32B)–C(31)–C(34B)	103.8(9)
Fe–C(25)–N(5)	175.9(4)	C(33B)–C(31)–C(34B)	118.0(9)
N(5)–C(26)–C(27)	107.2(4)	Fe–C(35)–N(7)	175.4(4)
N(5)–C(26)–C(28)	107.5(5)	N(7)–C(36)–C(37)	107.8(5)
N(5)–C(26)–C(29)	107.2(4)	N(7)–C(36)–C(38)	108.1(5)
C(27)–C(26)–C(28)	111.4(5)	N(7)–C(36)–C(39)	108.1(5)
C(27)–C(26)–C(29)	111.4(5)	C(37)–C(36)–C(38)	109.0(6)
C(28)–C(26)–C(29)	111.8(5)	C(37)–C(36)–C(39)	113.1(6)
Fe–C(30)–N(6)	173.0(4)	C(38)–C(36)–C(39)	110.5(6)
N(6)–C(31)–C(32A)	115.1(6)		

The structure clearly shows that two isothiocyanate molecules were involved in the product formation of **10cx**. One of these molecules has cycloadded over the C(17)=S(2) bond. The other isothiocyanate molecule is inserted with its C(8)–S(1) bond into the N(2)–Fe bond, whereby the N(2) atom is still coordinated to the Fe atom. The bond distance N(2)–Fe of 2.089(4) Å is normal for Fe–NC bonds [3,8]. The Fe–S(1)–C(8)–N(2) moiety does not form a perfect square, with angles of 71.39(10) (S–Fe–N), 78.92(15) (Fe–S–C), 93.2(2) (Fe–N–C), 107.2(2)° (S–C–N). The two sulphur atoms, S(1) and S(2) are coordinated to the Fe atom in a cis fashion. The structure also shows that one of the imine nitrogen atoms, i.e. N(3), is not coordinated to the Fe atom. Variable temperature ^{1}H NMR revealed that in solution there are two forms of **10**. Probably, the structure in Fig. 1 is of lower energy for this cycloadduct, i.e. the coordination of N(2) is energetically more favoured than the coordination of N(3) to the Fe atom. The geometry around Fe is slightly distorted octahedral. The mean angles around C(8) and C(17) (120°) reflect the change from sp to sp^2 hybridization. The Fe–S

bond lengths in complex **10cx** of 2.336(1) and 2.301(1) Å are comparable with analogous complexes [7,8].

2.4. Spectroscopic properties

The spectroscopic data (^{1}H-, ^{13}C-NMR and IR) of Fe(R–NC)$_3$([3.2.0]bic) (**10ax–dx, ay, cy**) and **11cy** are listed in Tables 4, 5 and 6 respectively; the atomic numbering is given in Scheme 2.

2.4.1. ^{1}H and ^{13}C NMR of 10

The ^{1}H NMR data are very similar to the known [2.2.2] bicyclic compounds [1–8] as far as the diazadiene part is concerned. The appearance of two resonances for the R″-groups, however, indicates that two isothiocyanate molecules are involved in the reaction sequence. For all complexes **10** with ligand **x**, the terminally coordinated tertiary butyl isocyanides **x** give three sharp resonances, indicating that these ligands do not interchange their positions on the NMR time scale.

The combination of two doublets with equal coupling constants in the regions 8.55–8.16 ppm (H(2)) and

Table 4
^{1}H NMR data [a] of complexes 10 and 11cy

Nucleus	Compound						
	10ax	10bx	10cx	10dx [b]	10ay	10cy	11cy
H(1)	4.29, d, 1H, 7.0 Hz	5.55 d, 1H, 5.5 Hz	4.25, d, 1H, 7.0 Hz	4.65, d, 1H, 5.4 Hz	4.35, d, 1H, 7.0 Hz	4.31, d, 1H, 7.0 Hz	4.42, d, 1H, 7.5 Hz
H(2)	8.55, d, 1H, 7.0 Hz	8.16, d, 1H, 5.6 Hz	8.55, d, 1H, 7.0 Hz	7.67, d, 1H, 5.4 Hz	8.60, d, 1H, 7.0 Hz	8.59, d, 1H, 7.0 Hz	2.58, d, 1H, 7.3 Hz
H(5)	3.88, sept, 1H, 6.7 Hz	5.30, sept, 1H, 6.7 Hz	3.87, sept, 1H, 6.7 Hz	5.58, sept, 1H, 6.8 Hz	3.67, sept, 1H, 7.1 Hz	3.51, sept, 1H, 6.3 Hz	4.49, sept, 1H, 6.5 Hz
H(6), H(7), H(8), H(10)	1.64, d, 3H, 6.5 Hz 1.39, d, 3H, 6.7 Hz 1.19, d, 3H, 6.2 Hz 1.14, d, 3H, 6.2 Hz	1.63, pst, 6H, 6.0 (6.5) Hz 1.40, d, 3H, 7.4 Hz 1.23, d, 3H, 6.6 Hz	1.61, d, 3H, 6.7 Hz 1.37, d, 3H, 6.5 Hz 1.17, d, 3H, 6.4 Hz 1.13, d, 3H, 6.3 Hz	1.42, d, 3H, 6.6 Hz 1.19, d, 3H, 6.8 Hz 1.12, d, 3H, 6.6 Hz 1.06, d, 3H, 3.1 Hz	1.65, d, 3H, 6.7 Hz 1.40, d, 3H, 6.5 Hz 1.19, d, 3H, 6.3 Hz 1.16, d, 3H, 6.3 Hz	1.37, d, 3H, 6.5 Hz 1.30, d, 3H, 6.7 Hz 1.19, d, 3H, 6.2 Hz 1.15, d, 3H, 6.2 Hz	1.80, d, 3H, 6.3 Hz 1.61, d, 3H, 6.6 Hz 1.02, d, 3H, 6.3 Hz 0.77, d, 3H, 6.2 Hz
H(9)	3.51, sept, 1H, 6.2 Hz	4.19, sept, 1H, 6.8 Hz	3.49, sept, 1H, 6.4 Hz	4.22, sept, 1H, 6.6 Hz	3.51, sept, 1H, 6.3 Hz	4.14, sept, 1H, 6.2 Hz	2.18, sept, 1H, 6.6 Hz
H(12), H(13), H(16), H(17)	7.35–6.80, m, 10H	7.20–6.72, m, 8H	7.20–6.70, m, 8H	8.24, d, 2H, 8.6 Hz 8.18, d, 3H, 8.7 Hz 7.35, d, 3H, 8.7 Hz 7.17, d, 3H, 8.6 Hz	7.33–6.90, m, 10H	7.17–6.79, m, 8H	7.26–6.70, m, 8H
R^2	1.55, s, 9H 1.50, s, 9H 1.29, s, 9H	1.46, s, 9H 1.33, s, 9H 1.14, s, 9H	1.53, s, 9H 1.48, s, 9H 1.30, s, 9H	0.98, s, 9H 0.94, s, 9H 0.89, s, 9H	3.92–3.78, m, 3H 1.94–1.25, m, 30H	3.95–3.87, m, 3H 1.83–1.12, m, 30H	3.65–3.43, m, 3H 1.95–1.08, m, 30H
R^3	see H(12), H(13), H(16), H(17)	2.31, s, 3H 2.27, s, 3H	3.75, s, 3H 3.74, s, 3H	—	see H(12), H(13), H(16), H(17)	3.76, s, 3H 3.74, s, 3H	3.80, s, 3H 3.79, s, 3H

[a] Chemical shifts are in ppm relative to Me$_4$Si; measured in CDCl$_3$ at 293 K and 300.13 MHz. [b] In C$_6$D$_6$.

Table 5
^{13}C NMR data [a] of complexes 10 and 11cy

Nucleus	Compound						
	10ax	10bx	10cx	10dx	10ay	10cy	11cy [b]
C(1)	61.0	61.4	60.6	61.7	60.6	60.5	53.0
C(2)	165.8	166.4	165.5	168.9	165.2	165.2	52.5
C(3), C(4)	180.1	180.2	179.7	183.6, 180.3	179.8	179.3	207.8, 181.8
C(5)	80.9	81.4	80.5	65.0	80.7	81.0	85.3
C(6), C(7),	25.0, 24.0,	25.4, 24.4,	24.6, 23.4,	23.1, 22.9,	24.5, 23.1,	24.5, 23.6,	22.8, 22.7,
C(8), C(10)	20.8, 20.4	21.2, 20.8	20.2, 19.8	22.6, 20.7	20.4, 19.9	20.5, 20.0	21.0, 19.4
C(9)	59.7	60.0	62.1	61.0	59.4	60.3	68.0
C(12), C(13),	129.1, 129.0,	130.2,	123.7, 123.2,	124.6,	129.4,	123.8,	123.6,
C(16), C(17)	123.5, 123.2,	130.0,	113.9, 113.8,	124.3,	128.6,	123.4,	123.0,
	122.8, 122.4	123.5, 123.2	113.3, 113.0	123.7,	128.4,	114.1,	115.7,
				122.1	123.0,	114.0	114.7,
					122.7, 122.4		113.9, 113.6
C(11), C(15)	155.1, 149.5	152.9, 147.3	156.0, 155.2	162.1, 160.8	154.5, 149.0	156.3,	159.3, 155.0
						155.5	
C(14), C(18)	see C(12),	132.7, 131.4	147.6, 142.0	142.8, 140.6	see C(12),	142.0,	146.9, 132.4
	C(13),				C(13),	140.9	
	C(16), C(17)				C(16),		
					C(17)		
R^2	58.0, 57.8,	58.3, 58.2,	57.3, 57.2,	57.5, 57.4,	54.8, 54.7,	54.8, 54.5,	54.9, 54.4,
	57.3, 31.0	57.6, 31.4	56.6, 30.3	30.3	54.5, 34.0–23.1	33.1–22.3	54.3, 35.7–25.4
R^2–NC	167.5, 167.3,	168.1 (br)	166.8, 166.1	168.9 (br)	167.0, 165.9	166.9,	169.4,
	166.8					166.7	168.6, 166.6
R^3	see C(12),	21.8	54.5	—	see C(12),	54.7, 54.6	55.8, 55.6
	C(13),				C(13), C(16),		
	C(16), C(17)				C(17)		

[a] Chemical shifts are in ppm relative to Me$_4$Si; measured in C$_6$D$_6$ at 293 K and 75.47 MHz.
[b] Measured in CDCl$_3$.

5.55–4.25 ppm (H(1)) shows that the products have an unreacted imine-group (H(2)) next to one that has been C–C coupled in the cycloaddition reaction, and therefore has been rehybridized to sp^3. Since one of the two imine groups is still intact, only one of the two isothiocyanate molecules can be involved in the cycloaddition reaction, while the other has to be inserted in the Fe–N bond. From the spectra it could not be deduced whether the second isothiocyanate molecule had inserted via its sulphur atom in the Fe–N bond or via the C=S or C=N bonds.

At room temperature the ^{1}H NMR spectra of compounds 10 in CD$_2$Cl$_2$ show only one set of sharp

signals for all protons (see Fig. 2(a)). Cooling a CD$_2$Cl$_2$ solution of 10ax to 273 K results in a broadening of the signal of H(5). At 253 K the signal of H(1) is broadened and the signal of H(5) has disappeared. At 243 K the

Table 6
IR data and mass data for the complexes 10 and 11cy

Compound	$\nu_{C\equiv N}$ (cm^{-1}) [a]	M [b]
10ax	2157.3 (s); 2111.4 (br)	716 (716)
10bx	2168.0 (s); 2135.4 (br)	744 (744)
10cx	2158.0 (s); 2115.3 (br)	776 (776)
10dx	2167.8 (s); 2132.2 (br)	—
10ay	2167.4 (s); 2121.1 (br)	793 (794)
10cy	2169.6 (s); 2125.1 (br)	853 (854)
11cy	2144.2 (s); 2102.1 (br)	853 (854)

[a] Recorded in CDCl$_3$.
[b] Observed (calculated) masses of the molecular ion (m/e); the M values are based upon the ^{56}Fe isotope; FAB ionization was used for complexes 10x and FD ionization for 10y and 11cy.
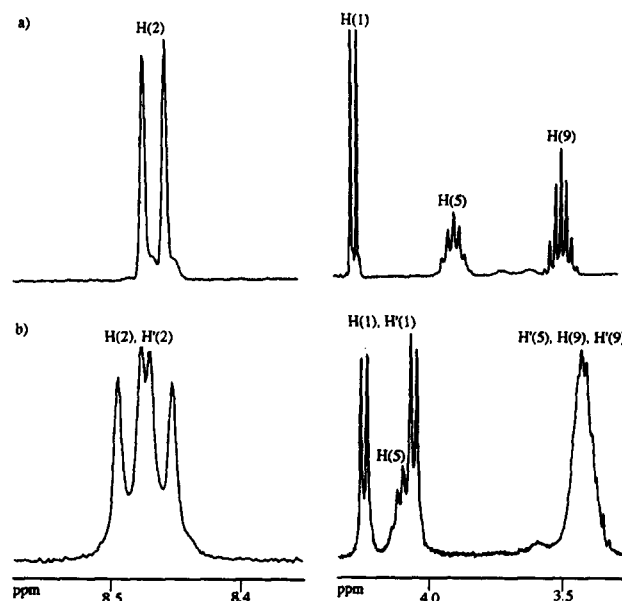

Fig. 2. Partial ^{1}H NMR of 10ax in CD$_2$Cl$_2$. resonances of H(1), H(2), H(5) and H(9): (a) at 298 K (fast exchange); (b) at 193 K (slow exchange).

signal of H(1) has almost disappeared. At 217 K resonances of two compounds are visible. Also the signals of the Me- (of ^{i}Pr) groups and the ^{t}Bu groups are broadened. The spectrum at 193 K (see Fig. 2) shows two sets of signals (primed and unprimed) of two compounds in a 1:1 ratio (H(1), H'(1): 4.25 ppm (7.2 Hz) and 4.10 ppm (7.2 Hz); H(2), H'(2): 8.48 ppm (7.2 Hz) and 8.45 ppm (6.7 Hz); H(5): 4.10 ppm (6.7 Hz); H'(5), H(9), H'(9): 3.42 ppm, broad; the rest of the signals overlap each other). Variable temperature NMR in toluene-d^8 leads to the same results. In both solvents the signals shift as a function of temperature, i.e. the observed chemical shifts in the room temperature spectra (fast exchange) are not equal to the population averaged value of the chemical shifts of these two compounds at 213 K, because all signals are continuously shifted to lower field on lowering the temperature. We interpret the dynamic behaviour as follows: in the slow exchange limit at low temperature we observe a frozen-in equilibrium mixture of the two isomers **10** and **10′** (see Scheme 3). It is not clear which set of signals belongs to which isomer. At room temperature the equilibrium is in the limit of fast exchange, i.e. the interconversion of the two isomers is too fast to observe them separately.

In the ^{13}C NMR spectra of **10**, the effect of rehybridization of one of the imine carbon atoms is reflected in a shift to higher field for the C–C coupled carbon nuclei (C(1)) next to the amino nitrogen. In all complexes, except **10bx** and **10dx**, the terminal isocyanide carbon nuclei are observed as sharp signals, which means that in these cases the isocyanides do not interchange their positions on the NMR time scale. At temperatures lower than 263 K the resonances of these nuclei become broadened.

Variable temperature ^{13}C NMR spectra of **10ax** show a dynamic behaviour consistent with the ^{1}H NMR results. Cooling down a sample of **10ax** in CDCl$_3$ to 263 K results in a broadening and a subsequent coalescence of the resonances of C(2), C(5)–C(7) and C(9). The compound is then still in the intermediate exchange, which means that the isomerization process is too fast on the NMR time scale to be completely frozen in.

2.4.2. ^1H and ^{13}C NMR of 11cy

There is some resemblance of the ^{1}H NMR spectrum of **11cy** with those of the earlier reported double cycloaddition products, Fe(THPP)(R$_{alkyl}$–NC)$_3$ [5]. Both complexes show a high field shift for the former imine hydrogen nuclei H(1) and H(2). However, in **11cy** one of the resonances is shifted to an even higher field than in the THPP complexes. The four methyl groups of the ^{i}Pr group are visible as four doublets, whereas the two MeO groups appear as two singlets. This inequivalence of the two isothiazol rings suggests that in **11cy** the FeL$_3$ fragment is probably unsymmetrically coordinated to only one of the amino-nitrogen atoms.

Both former imine carbon nuclei in complex **11cy** (C(1) and C(2)) are shifted to higher field, indicative of a rehybridization of the carbon atoms from sp^2 to sp^3. For the carbon nuclei C(3) and C(4) two different resonances are observed. For C(3) the resonance at 181.8 ppm is comparable with the shift value in complexes **10**. However, in **11cy** the resonance of C(4) is found at much lower field (207.8 ppm), which suggests that the FeL$_3$ unit is coordinated to the imine nitrogen or to the nitrogen-C(4) π-bond. Compared with the chemical shift of H(1), the resonance of H(2) is shifted to a remarkably low ppm value in complex **11cy**. This again suggests that the FeL$_3$ fragment is coordinated to the amino nitrogen atom next to C(2) and to the C(4)=N moiety. It may be that the FeL$_3$ fragment is coordinated in a delocalized fashion to the N–C(4)–C(2)–N moiety. This might explain a coalescence of the ^{13}C NMR signals of C(2) and C(5)–C(7) at low temperature. Coordination of one of the sulphur atoms to the iron atom is less likely but cannot be excluded.

2.4.3. IR

Complexes **10** show two ν(C–N) vibrations, one sharp resonance near 2160 cm^{-1}, and a very broad band
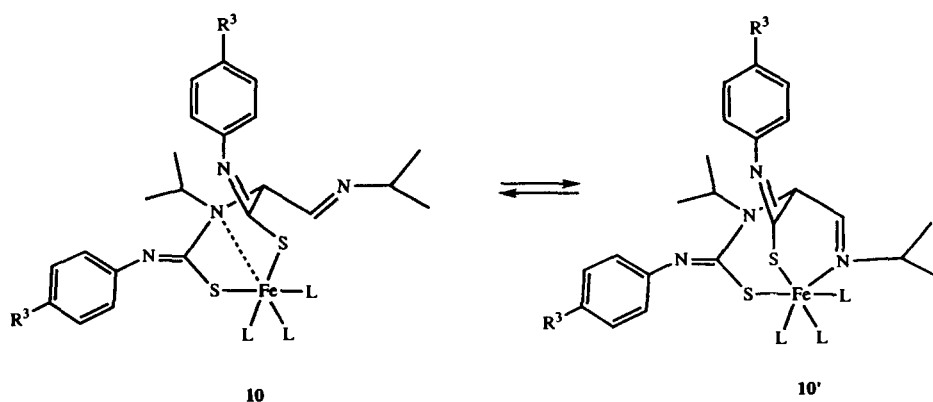
Scheme 3. Dynamic behaviour of complexes 10 in solution.

in the region 2111–2135 cm^{-1}. Compared with the IR data of the starting compounds 7 [5], complexes 10 show a shift to higher wavenumber, which reflects enhanced σ-donating/decreased π-backbonding character of the terminally coordinated isocyanides as a consequence of the iron atom being in the (+2) state due to the oxidative cycloaddition reaction.

The ν(C–N) vibrations in 11cy are shifted to lower wavenumbers compared with those of 10cy. This decrease in the σ-donating and an increase in the π-backbonding behaviour of the terminally coordinated isocyanides indicates that the iron atom has been reduced from Fe(+2) to the zero-valent state. Comparison of the higher wavenumbers of 11cy with those of 7y leads to the conclusion that the organic part of 11cy has more π-acceptor capacity than ^{i}Pr-DAB.

3. Conclusions

The reactions described in this paper show that aryl isothiocyanates not only react as dipolarophiles, but also insert in the Fe–N bond after the initial cycloaddition step. The insertion of the isothiocyanate takes place due to the failure of the terminally coordinated ^{t}Bu–NC ligands to insert.

On silica gel as reactive surface, complex 10cy converts to another complex 11cy in which two isothiocyanate molecules c have probably added with their C=S bonds across both Fe–N=C moieties of complex 7.

4. Experimental details

4.1. General information

Reactions were performed in an atmosphere of dry nitrogen using standard Schlenk techniques. Silica gel for column chromatography (silanized Kieselgel 60, 70–230 mesh, E. Merck, Darmstadt) was activated before use. Solvents were carefully dried and distilled prior to use. Elemental analyses were carried out by Dornis und Kolbe, Mikroanalytisches Laboratorium, Mülheim a.d. Ruhr, Germany. tert-Butyl isocyanide, cyclohexyl isocyanide and isothiocyanates a-d were purchased from Fluka and were used without further purification. Fe(R^2–NC)$_3$(^{i}Pr-DAB) (7) was prepared in situ from Fe(^{i}Pr-DAB)$_2$ and tert-butyl isocyanide according to published procedures [5,14].

4.2. Synthesis of Fe('Bu–NC)$_3$([3.2.0]bic) (10ax-dx)

To a solution of Fe(^{i}Pr-DAB)$_2$ (348 mg, 1.04 mmol) and 3.1 equiv. of tert-butyl isocyanide x (267 mg, 3.21 mmol) in 40 ml of hexane was added at −30°C 4

equiv. of isothiocyanates a–d. When the red colour of complex 7 had disappeared, the solution was slowly warmed up to room temperature. The yellow precipitate was then filtered off and washed with hexane, followed by extraction with 25 ml of diethyl ether. Addition of 20 ml of hexane to the Et$_2$O extract and cooling down to −20°C for 4 h gave a yellow-brown microcrystalline powder. The product was isolated, washed with 20 ml of hexane, and dried in vacuo to give 10ax-dx in yields of 30–50%.

Elemental analysis of 10ax: Found: C, 61.92; H, 7.55; N, 13.70. C$_{39}$H$_{57}$N$_7$O$_2$SFe. Calc.: C, 62.08; H, 7.47; N, 13.60%.

4.3. Synthesis of Fe(^{c}Hex–NC)$_3$([3.2.0]bic) (10ay, 10cy, 11cy)

To a solution of Fe(Pr^i-DAB)$_2$ (398 mg, 1.18 mmol) and 3.1 equiv. of cyclohexyl isocyanide y (401 mg, 3.67 mmol) in 40 ml of hexane was added at −30°C 4 equiv. of isothiocyanates a, c. When the red colour of complex 7 had disappeared, the solution was slowly warmed to room temperature. The yellow precipitate was then filtered off and washed with hexane, followed by extraction with 25 ml of diethyl ether. 10ay and 10cy were isolated in yields of 30–50% by drying in vacuo.

Column chromatography of 10cy gives an orange Et$_2$O fraction which gives 11cy after removal of the solvent and trituration with hexane as an orange viscous oil.

4.4. X-ray structure of complex 10cx

Crystals were grown from a saturated THF–Et$_2$O–hexane (1 : 1 : 1) solution at −20°C. An orange crystal (0.20 × 0.25 × 0.50 mm^3, cut to size and covered with inert oil) was mounted on a Lindemann glass capillary, and transferred into the cold nitrogen stream on an Enraf–Nonius CAD4-T diffractometer on rotating anode. Accurate unit-cell parameters and an orientation matrix were determined from the setting angles of 17 reflections (SET4 in the range 11.6 < θ < 13.6°) [10]. Reduced-cell calculations did not indicate higher lattice symmetry [16]. Crystal data and details on data collection and refinement are presented in Table 7.

Data were corrected for L_p effects and for a linear decay of 13% of the three periodically measured reference reflections. The structure was solved by automated direct methods (SIR-92) [17]. Refinement on F^2 was carried out by full-matrix least squares techniques (SHELXL-93) [18]; no observance criterion was applied during refinement. The tert-butyl on N(6) is disordered. A model was refined with constraints on the N(6)–methyl distances, the C(31)–methyl distances and the inter-methyl distances in the tert-butyl group. A con-

Table 7
Crystallographic data and details of data collection and refinement of 10cx

Crystal data	
Formula	$C_{39}H_{57}N_7O_2SFe$
Mol. wt.	775.91
Crystal system	triclinic
Space group	$P - 1$ (No. 2)
a, b, c (Å)	10.924(2), 13.871(3), 14.736(2)
α, β, γ (deg)	96.708(15), 93.070(12), 106.485(14)
V (Å^3)	2117.7(6)
Z	2
D_{calc} (g cm^{-3})	1.217
$F(000)$	828
μ (cm^{-1})	4.9
Crystal size (mm^3)	0.20×0.25×0.50
Data collection	
Temperature (K)	150
$\theta_{min}, \theta_{max}$ (deg)	1.4, 24.0
Wavelength (Mo K α) (Å)	0.71073 (graphite monochromator)
Scan type	$\omega/2\theta$
$\Delta\omega$, deg	$0.60 + 0.35 \tan \theta$
Horizontal, vertical aperture (mm)	3.00, 4.00
X-ray exposure time (h)	15.8
Linear decay (%)	13
Reference reflections	$2\,3\,-1, 1\,2\,-6, 4\,-4\,-2$
Data set	$0:12, -15:15, -16:16$
Total data	7053
Unique data	6653
Refinement	
No. of refined parameters	486
Final $R1$ [a], $wR2$ [b]	0.062 [$4603 F_o > 4\sigma(F_o)$], 0.167 (6653 data)
Goodness of fit	1.044
w^{-1} [c]	$\sigma^2(F^2) + (0.0923P)^2$
$(\Delta/\sigma)_{av}, (\Delta/\sigma)_{max}$	0.000, 0.001
Min and max resd dens. (e Å^{-3})	$-0.45, 0.74$

[a] $R1 = \Sigma \|F_o| - |F_c\| / \Sigma |F_o|$. [b] $wR2 = \{\Sigma[w(F_o^2 - F_c^2)^2 / \Sigma[w(F_o^2)^2]\}^{1/2}$.
[c] $P = (\max(F_o^2, 0) + 2F_c^2)/3$.

strained disorder model was also refined for the methoxy group C(24)–O(2). All non-hydrogen atoms were refined with anisotropic thermal parameters, except those of the disordered parts. The hydrogen atoms were refined with a fixed isotropic thermal parameter amounting to 1.5 or 1.2 times the value of the equivalent isotropic thermal parameter of their carrier atoms, for the methyl hydrogen atoms, and all other hydrogen atoms respectively.

Weights were optimized in the final refinement cycles. Positional parameters are listed in Table 1 for 10cx, bond distances in Table 2 and bond angles in Table 3. Neutral atom scattering factors and anomalous dispersion corrections were taken from International Tables for Crystallography [19]. Geometrical calcula-

tions and illustrations were performed with PLATON [20]; all calculations were performed on a DEC5000/125.

5. Supplementary material available

Table of atomic coordinates, bond lengths and angles and thermal parameters for 10cx have been deposited at the Cambridge Crystallographic Data Centre.

References

[1] H.-W. Frühauf, F. Seils, R.J. Goddard and M.J. Romão, *Organometallics, 4* (1985) 948.
[2] H.-W. Frühauf, F. Seils and C.H. Stam, *Organometallics, 8* (1989) 2338.
[3] M. van Wijnkoop, P.P.M. de Lange, H.-W. Frühauf, K. Vrieze, Y. Wang, K. Goubitz and C.H. Stam, *Organometallics, 11* (1992) 3607.
[4] P.P.M. de Lange, H.-W. Frühauf, M.J.A. Kraakman, M. van Wijnkoop, M. Kranenburg, A.H.J.P. Groot, K. Vrieze, J. Fraanje, Y. Wang and M. Numan, *Organometallics, 12* (1993) 417.
[5] P.P.M. de Lange, H.-W. Frühauf, K. Vrieze and K. Goubitz, *Organometallics, 12* (1993) 428.
[6] P.P.M. de Lange, R.P. de Boer, M. van Wijnkoop, J.M. Ernsting, H.-W. Frühauf, K. Vrieze, W.J.J. Smeets, A.L. Spek and K. Goubitz, *Organometallics, 12* (1993) 440.
[7] P.P.M. de Lange, E. Alberts, M. van Wijnkoop, H.-W. Frühauf, K. Vrieze, H. Kooijman and A.L. Spek, *J. Organomet. Chem., 465* (1994) 241.
[8] N. Feiken, H.-W. Frühauf, K. Vrieze, J. Fraanje and K. Goubitz, *Organometallics, 13* (1994) 2825.
[9] R. Sustmann, *Pure Appl. Chem., 40* (1974) 569.
[10] K.N. Houk and K. Yamaguchi, in A. Padwa (ed.), *1,3-dipolar Cycloaddition Chemistry*, Wiley, New York, 1984, Chapter 13.
[11] J. Cámpora, E. Gutiérrez, A. Monge, P. Palma, M.L. Poveda, C. Ruíz and E. Carmona, *Organometallics, 13* (1994) 1728.
[12] C. Mealli, R. Hoffmann and A. Stockis, *Inorg. Chem., 23* (1984) 56.
[13] R.D. Adams, L. Chen and W. Wu, *Organometallics, 12* (1993) 3812.
[14] H. tom Dieck and J. Dietrich, *Chem. Ber., 117* (1984) 694.
[15] J.L. de Boer and A.J.M. Duisenberg, *Acta Crystallogr. Sect. A40* (1984) C410.
[16] A.L. Spek, *J. Appl. Crystallogr., 21* (1988) 578.
[17] A. Altomare, G. Cascarano, C. Giacovazzo and A. Guagliardi, *J. Appl. Cryst., 26* (1993) 343.
[18] G.M. Sheldrick, SHELXL-93 *Program for crystal structure refinement,* 1993 (University of Göttingen, Germany).
[19] A.J.C. Wilson (ed.), *International Tables for Crystallography,* Vol. C, Kluwer, Dordrecht, 1992.
[20] A.L. Spek, *Acta Crystallogr., A Sect. 46* (1990) C34.